SST-forced Tropical Circulation Predictability in CWB Ensemble Hindcast

Jau-Ming Chen[1], Bin Wang,[2] Jyh-Wen Hwu[3], Ching-Feng Shih[3], Teh-Long Chang[1]

1. Institute of Navigation Science and Technology, National Kaohsiung Marine University, Taiwan

2. International Pacific Research Center, University of Hawaii, USA

3. Research and Development Center, Central Weather Bureau, Taiwan

Abstract

This study investigates the major SST sources of potential predictability and associated regulating processes for summer (June-August) low-level (850-mb) tropical circulations (30^0S-30^0N) using 1979-2003 ensemble hindcasts made by the CWB GFS model. Our analysis focuses on three tropical regions: the eastern Pacific Niño (EPN; 160^0E-80^0W), the western Pacific monsoon (WPM; 100^0E-160^0E), and the Indian Ocean monsoon (IOM; 40^0E-100^0E).

The WPM circulation tends to be coherent with the EPN circulation, and its predictability primarily comes from SST anomalies in the tropical eastern Pacific. On the other hand, the predictability of the IOM circulation is mainly attributed to SST anomalies in the tropical central Indian Ocean (IO). Strong SST anomalies tend to induce persistent and large-amplitude circulation anomalies and by so doing enhance potential predictability. Circulation predictability is generally higher over the WPM and EPN regions than over the IOM region.

Keywords: Predictability, SST, CWB GFS, Hindcast, Summer tropical circulation.

1. Introduction

Prediction of summer monsoon rainfall has been a great challenge in dynamic seasonal prediction. In the so-called two-tier prediction approach (Bengtsson et al. 1993), the AGCM rainfall anomalies were produced as a result of the AGCMs' passive response to the specified external SST forcing. However, in reality SST anomalies in the monsoon regions result in part from atmospheric forcing. Neglect of local monsoon-warm ocean interaction produces an erroneous local SST-rainfall relationship in the AGCM prediction (Wang et al. 2005). In an attempt to improve rainfall prediction, we turn to examination of the predictability of large-scale circulation anomalies. This was motivated by a previous work by Chen et al. (2005). They have demonstrated that summer rainfall variability in Taiwan and Southeast Asia is markedly influenced by the low-level (850 mb) circulation anomalies associated with the western North Pacific summer monsoon and the Pacific abrupt climate change during the late 1970s.

Conventional weather predictability focuses on the accuracy level of weather prediction. For climate predictability, it points to the potentially predictable components or the reproducibility of climate anomalies (e.g., Chen et al. 1997; Shukla et al. 2000; Kusunoki et al. 2001). In the AGCM ensemble prediction, the potentially predictable component is mainly caused by external SST forcing, while the unpredictable component results from model internal dynamic processes (e.g., Kumar et al. 1996; Rowell 1998; Kumar et al. 2001). Atmospheric climate predictability is inherently limited by the existence of unpredictable internal variability.

The main purpose of this study is to examine potential predictability of the summer (June-August) tropical low-level circulation from ensemble hindcasts conducted with the Central Weather Bureau (CWB) AGCM (namely, Global Forecast System, GFS). The focus regions include the eastern Pacific, the western Pacific, and the Indian monsoon regions. Low-level circulation is analyzed because it is a large-scale field closely connected to monsoon rainfall over East Asia. The major issues to be investigated are as follows:

- What are the major predictability features of the tropical circulations in the GFS hindcasts?
- How do external SST anomalies provide sources of predictability for these tropical circulations? What are the associated regulating processes?

2. Model and experimental designs

The CWB GFS is a global spectral primitive equation model with a T42 truncation and 18 vertical levels. Readers are referred to Liou et al. (1997) for more details of the dynamic and physical schemes used in the GFS. A 10-member ensemble hindcast is conducted with the GFS using an experimental design similar to that of the Seasonal-prediction Model Intercomparison Project (SMIP; Kusunoki et al. 2001). For the period of 1979-2003, 10 ensemble integrations were carried out for a length of seven months in each year, using initial conditions at 12 UTC from 21 April to 30 April of each year. The initial data used are derived from the National Centers for Environmental Prediction/Department of Energy reanalysis-2 (hereafter referred to as the RA-2) dataset (Kanamitsu et al. 2002) and the boundary conditions are the observed SSTs from the extended reconstructed SST (ERSST) dataset compiled by Smith and Reynolds (2003; 2004).

3. General predictive features

General predictive features of the GFS summer low-level circulation are illustrated by the signal-to-noise ratio of the 850-mb streamfunction (*S850*). The signal-to-noise ratio reveals that the potential predictability is large over the tropical western-central Pacific and small over the IO. To comply with the above predictive features, the tropical low-level circulation in the Indo-Pacific region is separated into three sections for analysis: the eastern Pacific Niño (EPN; 160^0E-80^0W, 30^0S-30^0N) region, the western Pacific monsoon (WPM; 100^0E-160^0E, 30^0S-30^0N) region, and the Indian Ocean monsoon (IOM; 40^0E-100^0E, 30^0S-30^0N) region. These three circulations are related to the ENSO, the Western Pacific-East Asian monsoon, and the Indian monsoon, respectively.

4. Predictability of GFS summer low-level tropical circulation

For the circulations over the EPN, WPM, and IOM regions, their 1979-2003 anomaly pattern correlation (APC) time series have a long-term mean of 0.59 in both the EPN and WPM regions and 0.40 in the IOM region. The reproducibility or potential predictability of the GFS tropical 850-mb circulation anomalies tends to be higher over the Pacific than over the IO.

The above APC time series have a simultaneous correlation coefficient of 0.69 between the EPN and WPM regions, 0.31 between the IOM and EPN regions, and 0.41 between the IOM and WPM regions. The WPM circulation tends to vary coherently with the predictability of the EPN circulation, rather than the IOM circulation. This feature suggests that consideration of predictability characteristics of the WPM and IOM circulations as an entity is not applicable to all models. The possible cause will be analyzed in the next section.

To specifically examine the spatial relationship between the potential predictability and the intensity of the SST anomaly, correlation patterns between the SST intensity (absolute value of SST anomaly, denoted as |SST|) and the APC time series of the three tropical circulations are computed. These significant patterns indicate that the potential predictability of the EPN and WPM circulations are mainly connected with |SST| in the tropical eastern Pacific, but only partially related to |SST| in the tropical western Pacific and the IO. For the IOM circulation, its potential predictability primarily links to |SST| in the tropical central IO , rather than in the tropical Pacific. It is clear that SST anomalies over the tropical eastern Pacific act as the major mechanism influencing potential predictability of the GFS summer low-level circulations over the Pacific, including both the EPN and WPM regions. Over the IO, the predictability of the IOM circulation is mainly regulated by SST anomalies in the tropical central IO.

5. Predictability source for the EPN and WPM circulations

This section investigates the sources of predictability in the GFS provided by SST anomalies for the summer tropical low-level circulations over the Pacific and the associated large-scale regulating processes. The EPN and WPM circulations tend to have a coherent APC variability. All summers in which these two circulations have the same predictability state are divided into four predictability types for analysis. There are 11 summers with the high predictability state. They are partitioned, in accordance with the phase of the Niño 3.4 SST anomaly, into the warm ($\geqq 0.5^0$C) and cold ($\leqq -0.5^0$C) phases, which are denoted as the APC(+)W and APC(+)C types, respectively.

The composite difference anomalies between the APC(+)W and APC(+)C types (warm minus cold) are analyzed in Fig. 1.. The SST difference anomalies exhibit an El Niño-like pattern. No noticeable SST anomaly is found in the tropical central and western IO. The east-west SST contrast in the Pacific forces a pair of tropical *X850* anomalies, consisting of a convergent (positive) center over the eastern Pacific and a divergent (negative) center over the western Pacific. In correspondence to this *X*850 anomaly pair, *S850* anomalies exhibit a Rossby-wave-like pattern, which features a pair of equatorial symmetric anomalous lows straddling the Equator over the western and central Pacific. This pattern spatially covers the regions of the EPN and WPM circulations and thus accounts for their coherent predictability. The corresponding vertical structure is an anomalous ψ_m cell across the Pacific (Fig. 4d), containing an ascending center in the EPN region (~155^0W) and a descending center in the WPM region (~130^0E). This ψ_m cell acts as an atmospheric bridge to convey the impacts of ENSO SST anomalies onto the EPN and WPM circulations simultaneously. This atmospheric bridge mechanism also helps to maintain a coherent predictability state for these two circulations.

6. Predictability source for the IOM circulation

The predictability states of the IOM circulation are categorized with two criteria: the APC value of the IOM circulation and SST value averaged over the tropical central IO (70^0-90^0E, 0^0-14^0S) where intensity of SST anomalies is significantly correlated with the APC value. The area-averaged SST value has a long-term mean of 27.7^0C and a standard deviation (SD) of 0.20^0C. A summer with an anomalous SST value larger/smaller than 0.16^0C/-0.16^0C (0.8 SD) is categorized as the anomalous warm/cold condition. The high predictability state has five/three summers concurrent with an anomalous warm/cold condition in the tropical central IO. The IOM circulation in the GFS hindcast tends to increase in predictability in accompany with the existence of strong SST anomalies in the tropical central IO. Its predictability source is analyzed next.

The composite difference anomalies between the APC(+)W and APC(+)C types (warm minus cold) of the IOM circulation are displayed in Fig. 2. The rectangular boxes indicate the spatial domains of the IOM circulation. SST anomalies are noticed by two major tropical warming centers in the IO and the tropical eastern Pacific.

These warm SST anomalies cause two anomalous convergent centers in the overlying *X850* anomalies. Two complementary and weak divergent anomalies occur in the Atlantic Ocean and the Maritime Continent, revealing a global wavenumber-2 structure. To the west of the convergent centers, the Rossby-wave response of tropical rotational circulation results in two meridional pairs of anomalous lows in *S850* anomaly,, a strong one over the IOM region and a moderate one over the western Pacific. The ψ_m anomalies along the Equator indicate that the strong IOM circulation anomalies directly link with anomalous upward motion and the convergent center over the tropical central IO. This suggests that the strong *in situ* SST anomalies in the tropical central IO act as the major predictability source for the IOM circulation in the APC(+)W and APC(+)C types.

7. Concluding remarks

The main purpose of this study is to examine the potential predictability of summer (June-August) 850-mb tropical circulation from a 10-member SMIP-type ensemble hindcast conducted for the period 1979-2003 with the Central Weather Bureau (CWB) Global Forecast System (GFS) model. The major tropical circulations are partitioned into three sub-regions for analysis: the eastern Pacific Niño (EPN; 160^0E-80^0W, 30^0S-30^0N) region, the western Pacific monsoon (WPM; 100^0E-160^0E, 30^0S-30^0N) region, and the Indian Ocean monsoon (IOM; 40^0E-100^0E, 30^0S-30^0N) region. The major predictability sources for these circulations and the associated regulating processes are investigated.

Analyses reveal three major predictability features for the GFS summer tropical low-level circulation. First, the potential predictability of the tropical circulation is generally higher over the Pacific than over the IO. Second, the predictability of the WPM circulation tends to vary from year to year in a coherent manner with the EPN circulation, but less coherently with the IOM circulation. This result suggests that the predictability of the WPM and IOM circulations should be examined separately. Third, the major predictability source for the EPN and WPM circulations is tropical SST anomalies in the eastern Pacific, while that for the IOM circulation is SST anomalies in the central IO. Stronger SST anomalies normally give rise to a higher predictability.

The predictability features of the summer tropical low-level circulation revealed in the present study are new but based on only one AGCM. It is not clear whether such predictability features are common to other AGCMs. To answer this question, future study is needed to analyze more AGCM experiments compiled by the model-intercomparison project.

Acknowledgements. This study was jointly supported by the Short-term Climate Prediction Project of the Central Weather Bureau, Taiwan, and National Science Council, Taiwan, under NSC 93-2625-Z-052-001 and NSC 94-2625-Z-052-001.

REFERENCES

Bengtsson, L., U. Schlese, E. Roeckner, M. Latif, T. P. Barnett, and N. Graham, 1993: A two-tier approach to climate forecasting. *Science*, **261**, 1026-1029.

Chen, J.-M., F.-C. Lu, S.-L. Kuo, and C.-F. Shih, 2005: Summer climate variability in Taiwan and associated large-scale processes. *J. Meteor. Soc. Japan*, **83**, 499-516.

Chen, W. Y., and H. M. Van den Dool, 1997: Atmospheric predictability of seasonal, annual, and decadal climate means and the role of ENSO cycle: A model study. *J. Climate*, **10**, 1236-1254.

Kanamitsu, M., and Coauthors, 2002: NCEP-DOE AMIP-II Reanalysis (R-2). *Bull. Amer. Meteor. Soc.*, **83**, 1631-1643.

Kumar, A., A. G. Barnston, M. P. Hoerling, 2001: Seasonal predictions, probabilistic verifications, and ensemble size. *J. Climate*, **14**, 1671-1676.

Kumar, A., M. Hoerling, M. Ji, A. Leetmaa, and P. Sardeshmukh, 1996: Assessing a GCM's suitability for making seasonal predictions. *J. Climate*, **9**, 115-129.

Kusunoki, S., M. Sugi, A. Kitoh, C. Kobayashi, and K. Takano, 2001: Atmospheric seasonal predictability experiments by the JMA AGCM. *J. Meteor. Soc. Japan*, **79**, 1183-1206.

Liou, C.-S., J.-H. Chen, C.-T. Terng, F.-J. Wang, C.-T. Fong, T. E. Rosmond, H.-C. Kuo, C.-H. Shiao, and M.-D. Cheng, 1997: The second-generation global forecast system at the Central Weather Bureau in Taiwan. *Wea. Forecasting*, **12**, 653-663.

Rowell, D. P., 1998: Assessing potential seasonal predictability with an ensemble of multi-decadal GCM simulations. *J. Climate*, **11**, 109-120.

Shukla, J., and Coauthors, 2000: Dynamic seasonal prediction. *Bull. Amer. Meteor. Soc.*, **81**, 2593-2606.

Smith, T. M., and R. W. Reynolds, 2003: Extended reconstruction of global sea surface temperatures Based on COADS data (1854-1997). *J. Climate*, **16**, 1495-1510.

Smith, T. M., and R. W. Reynolds, 2004: Improved extended reconstruction of SST (1854-1997). *J. Climate*, **17**, 12466-2477.

Wang, B., Q. Ding, X. Fu, I.-S. Kang, K. Jin, J. Shukla, F. Doblas-Reyes, 2005: Fundamental challenge in simulation and prediction of summer monsoon rainfall. *Geophys. Res. Lett.*, **32**, L15711.

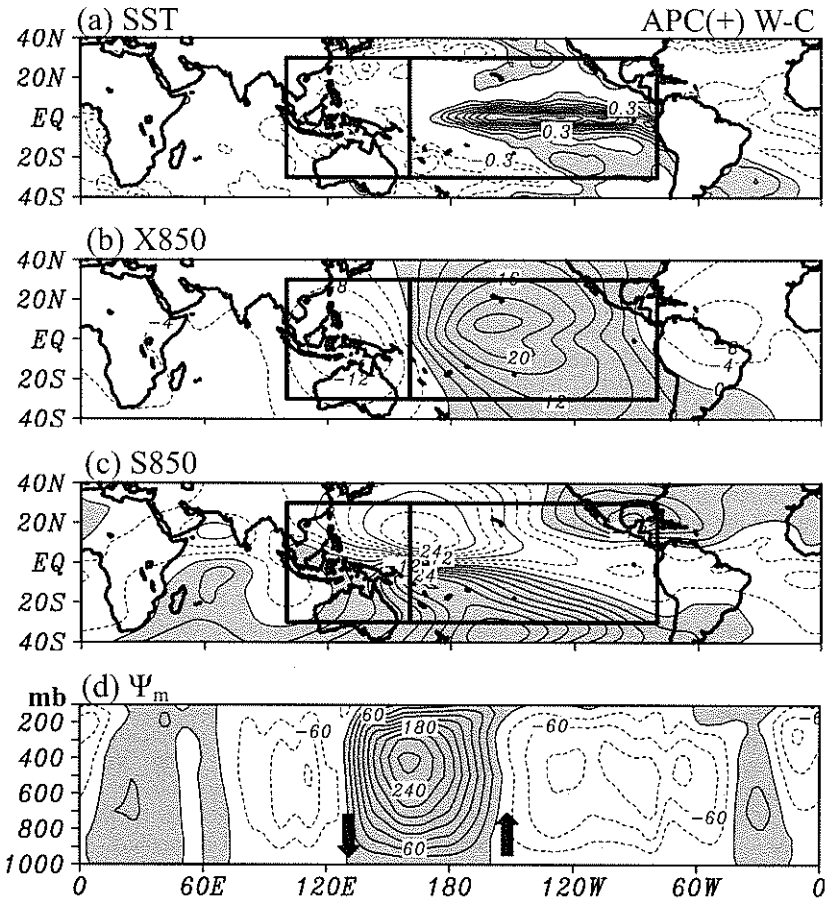

Figure 1: Composite difference anomalies of (a) SST, (b) 850-mb velocity potential, (c) 850-mb streamfunction, and (d) vertically-integrated mass flux function at the Equator between the APC(+)W and APC(+)C types (W minus C) of the EPN and WPM circulations. The contour intervals are 0.3^0C in (a), 4×10^5 m^2 s^{-1} in (b) and (c), and 30 m s^{-1} mb in (d). In (a), zero contour is suppressed. The shaded regions have the value larger than 0.3^0C. Positive values are shaded in (b), (c), and (d).

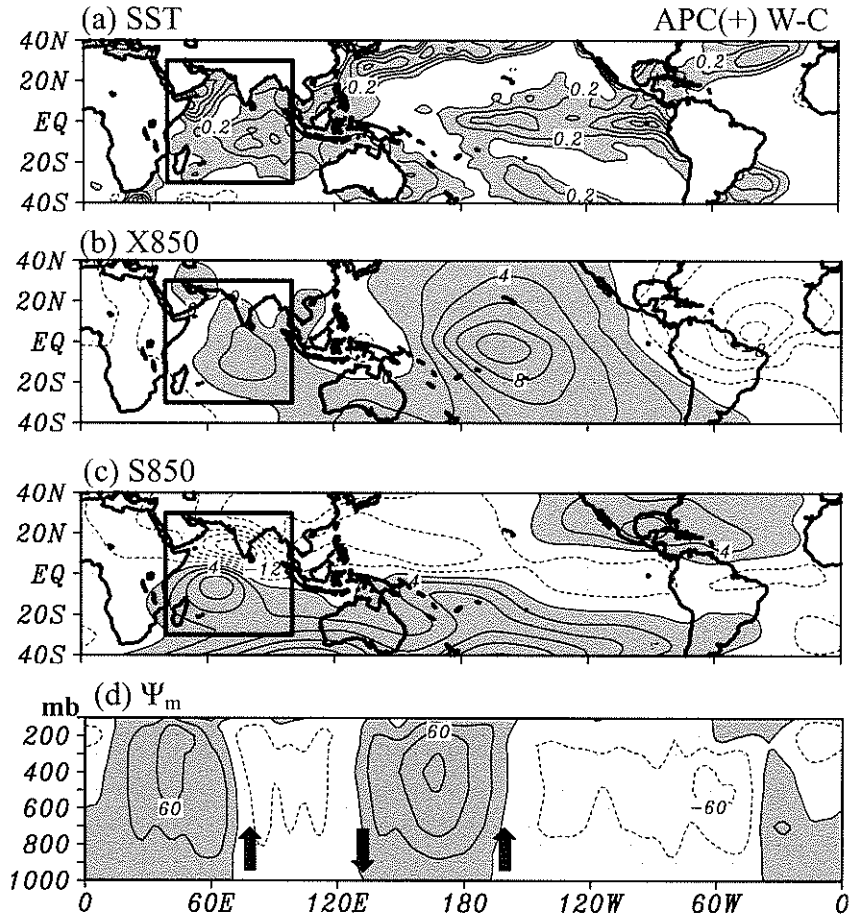

Figure 2: As in Fig. 1, except for the composite difference anomalies for the IOM circulation. The contour intervals are 0.1^0C in (a) and 2 x 10^5 $m^2 s^{-1}$ in (b). The shaded regions in (a) have the value larger than 0.1^0C.